Theoretical electronic structures and relative stabilities of the spinel oxynitrides M_3NO_3 (M=B, Al, Ga, In)

Onyekwelu U. Okeke and J. E. Lowther
DST/NRF Center of Excellence in Strong Materials and School of Physics, University of the Witwatersrands, P. O. Wits, Johannesburg 2050, South Africa

(Received 16 August 2007; revised manuscript received 11 December 2007; published 25 March 2008)

A spinel structure of an oxynitride material in the form M_3NO_3 (M=B, Al, Ga, or In) is considered to be derived from a reaction of the form $MN+M_2O_3 \rightarrow M_3NO_3$. Various possible phases of MN and M_2O_3, which could lead to the M_3NO_3 spinel material, are considered. The spinels containing B and Al exhibit higher resistance to compression and shear than those containing Ga and In, and these are suggested to be potentially important hard materials possibly formed under extreme conditions. Calculated energetics of the proposed reaction favor the formation of spinels containing Ga and In with such materials having potentially significant optoelectronic applications.

DOI: 10.1103/PhysRevB.77.094129 PACS number(s): 71.15.Nc, 77.84.Bw, 81.05.Zx

I. INTRODUCTION

Spinel is one of the known gemstones in an oxide class. These materials exhibit remarkable electrical, magnetic, and other physical characteristics, such as large specific gravity of 3.5–4.1, possess an intermediate to high refractive index, show good dispersion, and are available in many colors. The spinel structure is named after the class of mineral spinel known as $MgAl_2O_4$, which represents the spinel group. $MgAl_2O_4$ has a lattice parameter, a=8.0898 Å, and is a ceramic oxide that is characterized with good optical and insulating features. It has shown strong radiation resistance to amorphization and formation of defect clusters and dislocation loops due to the large number of cation sites.[1,2]

More generally, the spinel structure refers to the class of oxides with chemical formula AB_2O_4, where A and B are either divalent (+2) and trivalent (+3) or tetravalent (+4) and divalent cations. This structure has a cubic closed packing (fcc) arrangement of oxide ions with a large unit cell containing 8 f.u. The unit cell of a spinel ($A_8B_{16}O_{32}$) contains 56 atoms (i.e., 8 A, 16 B, and 32 oxygen atoms), and the spinel belongs to the space group of $Fd3m$ with an internal parameter u for the anion known as the oxygen parameter.[3,4] Besides the spinel-type oxides, some halides, nitrides, and sulfides also crystallize in the spinel structure. Most notable of these are Si_3N_4 and Co_3S_4. The cation to anion ratio distribution of such spinels is 3:4, irrespective of the many different phases such as binary (Fe_3O_4), ternary ($MgAl_2O_4$), and quaternary phases ($Si_{6-z}Al_zO_zN_{8-z}$).[5] Si_3N_4, in particular, is an important new synthetic hard material recently found in the spinel structure.[6–9]

Computer modeling of novel hard or superhard materials has been a driving issue in the research of new materials[10] and provides valuable insight into potentially important new materials and similar materials that may not be important. Hard materials, especially, are of great interest due to their superior mechanical and chemical properties, such as higher compression strength, thermal conductivity, spectral transmittances, hole mobilities, refractive index, and chemical stability.[11] They usually possess a strongly covalent bonded crystal structure often of high symmetry. The properties of hard materials strongly depend on many parameters, such as pressure, temperature, porosity, impurities, dislocations, and hardness, which are often correlated to various other physical properties, such as ionicity, melting point, band gap, elastic modulus, and cohesive energy.[12,13] Hard materials have been used as gemstones, heat sinks, radiation windows, speaker component, mechanical bearings, surgical knives, container coatings, and, potentially, novel semiconductors. One of the major industrial applications of hard materials is as superabrasives.[13]

There has been much experimental and theoretical efforts devoted in recent years to develop a new class of hard materials with properties that can compete and even have properties superior to diamond or cubic boron nitride (c-BN)—which are the two well-known superhard materials. Spinel structures have notably been found to be potentially important hard materials.[10] The high hardness and high density that characterized a spinel is because of the tetrahedral bonded nature of the coordinated cations that is similar to that of diamond, the hardest known bulk material.[14] The hardness of a material is decided by the process of how resistant the interatomic bonds in the material are against distortions needed to generate deformations and, in part, how defects such as dislocation can move in the system. There are two major hardness measuring techniques of hardness: a Vickers test uses a symmetric diamond tip and a Knoop test uses an asymmetric diamond tip.[15,16]

In this work, we examine a spinel structure of compounds formed from group-III oxides and nitrides leading to the spinel structure with a chemical formula M_3NO_3. The electronic structure, equation of state, elastic constants, and stabilities of possible synthesis phases will be investigated. Essentially, the chemical equation that we shall consider to represent the formation of the spinel structure is

$$M_2O_3 + MN \rightarrow M_3NO_3,$$

where, in the present work, M can represent boron, aluminium, gallium, or indium. The left side of the equation represents several possible forms of the group-III oxides and nitrides.

First, we review the constituent parent phases of materials that are the essential building blocks of the spinels, and then we present an analysis of the optimized geometries, crystal structures, bulk modulus, as well as their relative stabilities. We also examine the elastic constants of the spinel structure and the properties of the material to shear.

II. CRYSTAL STRUCTURE OF SPINEL

In the spinel structure, the cubic closed-packed array of anions holds two types of voids or interstices, namely, the tetrahedral and the octahedral interstices. The tetrahedral site is formed by four lattice atoms and is commonly denoted as the A site, whereas the octahedral is formed by six lattice atoms of the octahedron and is commonly denoted as the B site. The relative ionicity (i.e., the ionic radius) and the size of the interstices determine how the cations occupy the site with a tetrahedral or octahedral symmetry.[17,18] In the unit cell of the spinel, there are a total of 64 tetrahedral interstices and 32 octahedral interstices between the anions; however, only 8 and 16 of the tetrahedral and octahedral sites are occupied by the cations, respectively. In other words, $\frac{1}{8}$ of the A sites and $\frac{1}{2}$ of the B sites are occupied by the cations. The tetrahedrally coordinated cations form a diamond cubic sublattice with a repeat unit equal to the lattice parameter. This explains the relatively high hardness and high density that is typical of spinel.

The position of the cations are fixed by the symmetry of the structure, but the anion positions are variable and are specified by the oxygen parameter u. The oxygen parameter u is the distance between the oxygen ion and the face of the cube edge along the cube diagonal of the spinel subcell. For instance, when the A sites are too small for the cations, the oxygen ions move slightly to accommodate them and tend to shrink the size of the B site by the same amount as the A site expands. In all spinel-like structures, the oxygen parameter u has a value about 0.375. However, in actual spinel lattices, this ideal pattern is slightly deformed, usually corresponding to $u > 0.375$, so the oxygen tetrahedron in the A cubes is somewhat expanded and the oxygen octahedron in the B cubes is contracted. Accordingly, in that case, the octahedrons formed by the six oxide ions directly surrounding the positive ions in the B cubes deviate from the regular octahedrons.[17]

There are two types of limiting configurations of cations in the spinel-structured compounds called normal (or direct) spinel and inverse (or indirect) spinel. The normal spinel refers to a compound that is composed of divalent and trivalent cations, where the less abundant divalent cations occupy tetrahedral A sites and the more abundant trivalent cations occupy the octahedral B sites. However, the work done by Barth and Posnjak,[19] who based their conclusions on a detailed discussion of the intensities of x-ray diffraction pictures, pointed out a second possibility called the inverse spinel, $B(AB)O_4$, which is composed of tetravalent and divalent cations, where half of the divalent cations occupy tetrahedral A sites and all the tetravalent cations together with the other half of the divalent cations occupy the octahedral B sites.[17,20]

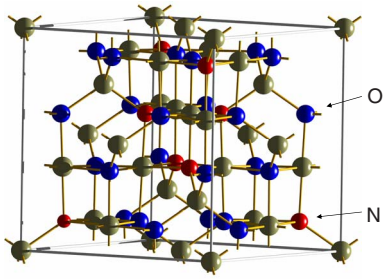

FIG. 1. (Color online) The cubic unit cell of the M_3O_3N spinel structure. N atoms are at a tetrahedral position inside the cubic unit cell.

Besides these two arrangements, there are possibilities for some intermediate arrangements of the form $(A_{1-2\lambda}B_{2\lambda})(A_{2\lambda}B_{2-2\lambda})O_4$ with an average distribution of all ions about the spinel cation positions. Spinels with these configurations are known as the intermediate or random spinels. They are located somewhere between the normal and the inverse arrangements. The variable λ is the so-called inversion parameter, which specifies the fraction of A sites occupied by the majority of ions. It ranges from 0 for the normal spinel to 0.5 for the inverse spinel.[21] In addition, there are ternary spinels of the type $A_xB_2S_4$, where A=Al and Ga and B=Mo, V, and Cr,[22] or quaternary spinels with Si, Al, O, or N.[23,24] Thus, we see that the structure that is called spinel is highly variable both chemically, stoichiometrically, as well as topologically. An essential structure of the spinels is that they are composed of either a 12-fold or a fourfold degenerate symmetry site depending on the occupancy of the octahedral or tetrahedral interstices.

In this work, we are to consider a specific spinel structure for the stoichiometry M_3NO_3 and use the 56-atom unit cell as is commonly used for the spinel structure. Nominally, the symmetry of this spinel structure is $P\bar{4}3m$, and this is shown in Fig. 1. As shown in the figure, the most significant element in this cubic unit cell consists of N atoms arranged in a tetrahedral symmetry about the center of the 56-atom unit cell. This structure is unique because of the symmetry of the N atoms, and as such has no normal or inversion character, as discussed earlier for the other spinels, which is appropriate. The structure has been observed in the recently synthesized Ga_3NO_3 system.[25,26]

III. SPINELS AND GROUP-III OXIDES AND NITRIDES

If we are to synthesize the M_3NO_3 spinel structure, then we start from oxide or nitride phases. The oxide or nitride materials exist in two or more crystallographic phases, which can be stable or metastable polytypes. The phases of the group-III oxides and nitrides are described as follows.

A. Group-III oxides

The suggested oxides of group-III elements (atoms) are B_2O_3, Al_2O_3, Ga_2O_3, and In_2O_3, which are to be considered.

1. Boron oxide (B_2O_3)

Boron oxide (B_2O_3) is an important industrial mineral. It has excellent properties, such as hardness, insulation, and linear and nonlinear optical behaviors, which have made them useful for various electronic and optoelectronic devices. Boron oxide can be produced by a direct reaction of boron and oxygen under pressure. It has the advantage of very low heat expansion, high refractive index, and high ion conductivity. Because of these characteristics, boron oxide is used widely in glass forming materials after silica. When doped on ceramic materials, it enhances conductivity and structural stability.[27,28] B_2O_3 is also one of the additives used to modify textural and acid based properties of metal oxides, such as Al_2O_3, Ti_2O_3, and MgO.[29]

The structure of B_2O_3 has been a subject of debate for many years now. However, because of many spectroscopic investigations such as neutron and x-ray diffraction, Raman spectroscopy, as well as NMR and NQR spectroscopies, it has been widely viewed and accepted that boron oxide is a network of oxygen-sharing BO_3 triangles. Three BO_3 triangles combine to form a mixed random network of boroxol rings B_3O_6.[30–33] A model of vitreous B_2O_3 with boron atoms residing in the boroxol rings has two polymorphs in which the boron atoms have different coordination numbers, in which the B atoms are trigonally and tetrahedrally coordinated by O atoms. They are B_2O_3-I and B_2O_3-II. B_2O_3-I is known as the low-pressure structure of B_2O_3, obtained at a pressure of 2 GPa with a hexagonal unit cell. It crystallizes in space group $P3_1$ with $a=4.336$ and $c=8.340$ Å, as reported by Gurr *et al.*[34] B_2O_3-II is the high-pressure phase structure of B_2O_3 obtained at a pressure of 6.5 GPa and a temperature of 1100 °C. The structure of B_2O_3-II is orthorhombic with $a=4.613$, $b=7.803$, and $c=4.129$ Å and space group $Ccm2$, built up by two sets of tetrahedral with shared corners as described by Prewitt and Shannon.[35] It could be observed that under pressure, crystal B_2O_3 undergoes a structural transformation that increases the boron coordination from a BO_3 triangular unit into a BO_4 tetrahedral unit.[36]

2. Aluminum oxide (Al_2O_3)

Aluminum oxide or alumina has a unique range of industrial applications as structural ceramic and optical materials. It is extensively used as a high temperature, corrosion resistant refractory material due to its hardness, chemical durability, abrasive resistance, mechanical strength, high surface area, and good electrical insulation. Alumina exists in two major crystallographic phases known as the stable or ground state structure and the metastable or transition structures. The stable phase is commonly known as corundum (α-Al_2O_3), which has the hexagonal closed packed (hcp) rhombohedral crystal structure with the stacking sequence *ABAB* and lattice parameter $a_0=4.76$ Å and $c_0=12.99$ Å.[37] θ-Al_2O_3 is another form of alumina to be considered, which has a monoclinic structure with symmetry $C2/m$.[38]

3. Gallium oxide (Ga_2O_3)

Gallium oxide is thermally and chemically stable with insulating properties at room temperature but semiconducting at higher temperatures. Ga_2O_3 has several polymorphs, but the two major forms are α and β, which can be classified under high- and low-temperature conditions. High-temperature β-Ga_2O_3 is the most stable form of the metal oxide. It has a monoclinic structure with a space group $C2/m$ and contains both octahedral and tetrahedral cation sites in equal quantities. It has a wide band gap energy of about $E_g=4.8$ eV. α-Ga_2O_3 is the low-temperature phase of gallium oxide with a rhombohedral structure. The phase transition temperature from α-Ga_2O_3 to β-Ga_2O_3 is about 600 °C. α-Ga_2O_3 thus has the strong advantage of low synthesis temperature as compared to that of β-Ga_2O_3.[39,40]

TABLE I. Cell structures of BN, B_2O_3, and B_3NO_3 and AlN, Al_2O_3, and Al_3NO_3.

Phase	Space group	Lattice (Å) LDA (GGA)	Expt. (Å)
c-BN	$P\bar{4}3m$	3.746 (3.626)	3.615[a]
B_2O_3-I	$P3_1$	$a=10.578$ (11.161)	
		$b=2.420$ (2.420)	
		$c=4.729$ (4.764)	
B_2O_3-II	$Ccm2_1$	$a=4.582$ (5.062)	$a=4.613$[b]
		$b=7.780$ (7.103)	$b=7.803$[b]
		$c=4.102$ (4.455)	$c=4.129$[b]
B_3NO_3	$P\bar{4}3m$	$a=6.842$ (6.947)	
w-AlN	$P6_3mc$	$a=3.091$ (3.128)	$a=3.111$[a]
		$c=4.945$ (5.012)	$c=4.978$[a]
c-AlN	$F\bar{4}3m$	$a=4.346$ (4.400)	$a=4.380$[c]
α-Al_2O_3	$R\bar{3}c$	$a=4.733$ (4.805)	$a=4.761$[d]
		$c=12.908$ (13.123)	$c=12.995$[d]
θ-Al_2O_3	$C2/m$	$a=11.695$ (11.911)	$a=11.80$[e]
		$b=2.895$ (2.938)	$b=2.910$[e]
		$c=5.593$ (5.669)	$c=5.621$[e]
Al_3NO_3	$P\bar{4}3m$	$a=7.937$ (8.057)	

[a]Reference 54.
[b]Reference 35.
[c]Reference 44.
[d]Reference 55.
[e]Reference 56.

4. Indium oxide (In_2O_3)

Indium oxide is also a wide band gap semiconductor with an energy gap $E_g \sim 3.70$ eV. It has been widely used as a material for transparent electrodes in electronic devices such as liquid crystal displays and solar cells, as a barrier layer in tunnel junctions, as a sensing material in gas sensors, and as a material in nanowire technology. In_2O_3 exists in two crystal phases, namely, the body-centered cubic (bcc) and the rhombohedral (rh) structures. The bcc-In_2O_3 has a cubic cell lattice constant of $a=10.118$ Å, and the symmetry of the unit cell is $Ia3$, whereas the rh-In_2O_3 lattice constants are $a=5.478$ Å and $c=14.51$ Å, with symmetry R-3C.[41] The

TABLE II. Cell structures of GaN, Ga_2O_3, and Ga_3NO_3 and InN, In_2O_3, and In_3NO_3.

Phase	Space group	Lattice (Å) LDA (GGA)	Expt. (Å)
w-GnN	$P6_3mc$	a=3.184 (3.211)	a=3.180[a]
		c=5.178 (5.231)	c=5.166[a]
c-GaN	$F\bar{4}3m$	a=4.499 (4.538)	a=4.50[b]
α-Ga_2O_3	$R\bar{3}c$	a=4.978 (5.060)	
		c=13.351 (13.602)	
β-Ga_2O_3	$C2/m$	a=12.162 (12.445)	a=12.230[c]
		b=3.033 (3.083)	b=3.040[c]
		c=5.801 (5.876)	c=5.80[c]
Ga_3NO_3	$P\bar{4}3m$	a=8.267 (8.425)	a=8.20[c]
w-InN	$P6_3mc$	a=3.505 (3.585)	a=3.533[a]
		c=5.668 (5.787)	c=5.166[a]
c-InN	$F\bar{4}3m$	a=4.941 (5.046)	a=4.980[b]
rh-In_2O_3	$R\bar{3}c$	a=13.349 (13.068)	
		b=3.320 (3.472)	
		c=6.158 (6.687)	
bcc-In_2O_3	$Ia3$	a=10.027 (10.337)	a=10.118[d]
In_3NO_3	$P\bar{4}3m$	a=9.037 (9.285)	

[a]Reference 54.
[b]Reference 44.
[c]Reference 25.
[d]Reference 41.

physical and optical properties of bcc-In_2O_3 have been reported,[41] whereas for rh-In_2O_3, no information is available.

B. Group-III nitrides

The group-III nitrides, namely, BN, AlN, GaN, and InN, are currently being investigated for their unique potential. They have uses in high-temperature, high-power, and high-frequency electronics and are materials that are characterized by large band gaps and strong mixed ionic and covalent bonding. Furthermore, the properties of their zinc-blende and/or wurtzite phase, such as hardness, high melting point, high thermal conductivity, and large bulk moduli, also make them useful for protective coatings. Apart from BN, the group-III nitrides crystallize into two forms or phases, namely, the stable wurtzite structure and the metastable sphalerite or zinc blende that is normally regarded as a cubic structure. BN has hexagonal and cubic phases that are similar to graphite and diamond.[42–44] Among all the phases, cubic BN (which has a zinc-blende structure) is the most interesting, both technologically and scientifically. *c*-BN is the second hardest material known after diamond and has excellent thermal conductivity. It can form both *n*- and *p*-type semiconductors when doped appropriately.[45] Aluminum nitride (AlN) is unique for its ultrahigh direct gap of more than 6 eV as well as the ability of the band gap engineering by alloying and forming heterostructures with GaN.[46]

TABLE III. LDA and GGA estimated values of zero-pressure energy, equilibrium volume, and bulk moduli of the ambient phases of the various materials. The GGA results are in parentheses.

Material	E_0 (eV/atom)	V_0 (Å^3)	B_0 (GPa)
c-BN	−9.715 (−8.710)	38.79 (31.66)	404 (475)
B_2O_3-I	−8.439 (−7.456)	39.90 (41.25)	322 (299)
B_2O_3-II	−8.925 (−7.720)	49.45 (53.77)	177 (182)
B_3NO_3	−8.398 (−7.382)	38.61 (40.51)	339 (294)
w-AlN	−8.213 (−7.445)	69.13 (71.79)	211 (194)
c-AlN	−8.190 (−7.423)	69.30 (71.94)	212 (193)
α-Al_2O_3	−8.312 (−7.480)	56.39 (59.13)	258 (230)
θ-Al_2O_3	−8.262 (−7.471)	62.08 (65.19)	206 (185)
Al_3NO_3	−8.211 (−7.398)	60.32 (63.16)	233 (208)
w-GaN	−6.973 (−6.157)	76.98 (79.23)	212 (170)
c-GaN	−6.965 (−6.152)	77.02 (79.28)	212 (170)
α-Ga_2O_3	−6.904 (−6.004)	64.69 (68.01)	262 (198)
β-Ga_2O_3	−6.866 (−6.035)	70.61 (74.07)	192 (155)
Ga_3NO_3	−6.854 (−5.986)	57.67 (72.21)	232 (177)
Ga_3NO_3	−6.874[a] (−6.209)[b]	69.54[a] (72.30[b])	210[b]
w-InN	−6.176 (−5.446)	101.86 (108.46)	135 (121)
c-InN	−6.175 (−5.434)	101.26 (103.10)	163 (132)
rh-In_2O_3	−6.366 (−5.480)	90.47 (97.00)	123 (98)
c-In_2O_3	−6.512 (−5.607)	85.13 (93.57)	172 (156)
In_3NO_3	−6.366 (−5.455)	89.00 (98.26)	163 (145)

[a]Previous theoretical results for Ga_3NO_3 from Ref. 58.
[b]Previous theoretical results for Ga_3NO_3 from Ref. 59.

The nitrides of Ga and In are equally important. GaN is a wide band gap wurtzite structure used for optoelectronic and high-frequency devices in the wavelength ranging from blue-green to ultraviolet. On the other hand, InN and its alloys have also emerged as promising materials for optoelectronic devices, such as light-emitting diodes and solar cells.[47,48]

IV. CALCULATIONS AND RESULTS

Calculations of the optimized geometries, relative stabilities, as well as their equilibrium properties were performed

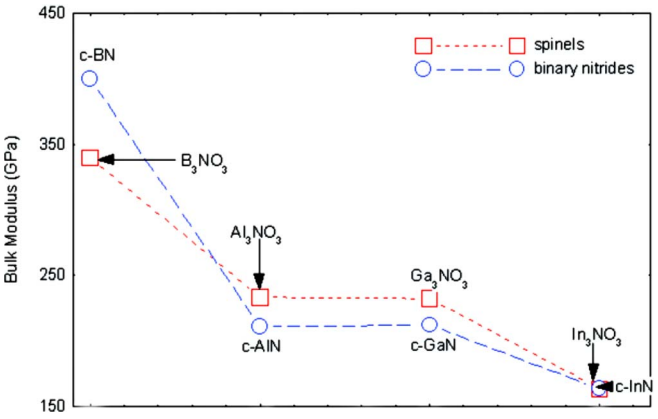

FIG. 2. (Color online) Equation of state derived bulk modulus, LDA results.

TABLE IV. Calculated elastic constants and effective (Voigt) isotropic elastic modulii for spinel oxynitrides. Experimental values for diamond are B=442–433, G=524–544, E=1142–1164, and ν=0.1. For spinel Si_3N_4 B=308 and G=258. All elastic moduli are in GPa.

	Spinel	$c_{1,1}$	$c_{1,2}$	$c_{4,4}$	B	G	E	ν
LDA	B_3NO_3	190	418	415	342	203	508	0.25
	Al_3NO_3	344	179	184	234	143	357	0.25
	Ga_3NO_3	316	202	131	240	101	266	0.32
	In_3NO_3	212	136	76	161	61	162	0.33
GGA	B_2NO_3	72	414	361	300	148	381	0.29
	Al_3NO_3	310	160	175	210	135	333	0.24
	Ga_3NO_3	249	146	124	180	95	242	0.28
	In_3NO_3	202	138	65	159	52	140	0.35

within the density functional theory. The computational approach uses projector augmented wave potentials[49] and a plane wave formalism with a local density approximation (LDA), as parametrized by Perdew and Zunger,[50] and a generalized gradient approximation (GGA),[51] as carried out through the VASP electronic structure code.[52] Integration over the Brillouin zone is done on a special K-point samplings on a Monkhorst-Pack grid[53] with an energy cutoff of 500 eV. The special K-point samplings used are on $4\times4\times4$ and $8\times8\times8$ for the spinels and the group-III oxides and nitrides, respectively, to ensure satisfactory convergence. This gave an estimated calculational error in the total energy of 0.05 eV/atom.

A. Structural properties

The calculated optimized structures for all the spinels and the group-III oxides and nitrides (as well as the respective phases) are shown in Tables I and II. Table I shows the optimized calculated structural parameters for BN, B_2O_3, and B_3NO_3 and AlN, Al_2O_3, and Al_3NO_3, and Table II the cell structures of GaN, Ga_2O_3, and Ga_3NO_3 and InN, In_2O_3, and In_3NO_3. Both LDA and GGA results are in good agreement with the experimental results aside from the value of the c axis of w-InN, and this experimental value possibly needs further examination.

TABLE V. ΔE_{stab} values for LDA and GGA (in parentheses). *denotes the lowest value of ΔE_{stab} for the phases indicated.

Spinel	Oxide	Nitride	
			c-BN
B_3NO_3	B_2O_3-I		0.405* (0.434)*
	B_2O_3-II		0.753 (0.622)
		w-AlN	c-AlN
Al_3NO_3	α-Al_2O_3	0.053 (0.060)	0.067 (0.065)
	θ-Al_2O_3	0.017* (0.053)*	0.031 (0.059)
		w-GaN	c-GaN
Ga_3NO_3	α-Ga_2O_3	0.046 (0.062)	0.068 (0.062)
	β-Ga_2O_3	0.019* (0.083)	0.041 (0.083)
		w-InN	c-InN
In_3NO_3	rh-In_2O_3	−0.054 (0.022)	−0.054* (0.018)*
	bcc-In_2O_3	0.052 (0.106)	0.051 (0.103)

B. Equation of state bulk modulus

The bulk modulus of a material measures its resistance to volume reduction under compression. The upper limit of bulk modulus of a material reflects the intrinsic compressive hardness of the crystal structure.[13] An estimate of the bulk modulus was obtained using the first-order Birch equation of state,[57] as obtained from a calculation of the total energy as a function of the cell volume. The results are summarized in Table III.

The trend in the equilibrium volume and the bulk modulus is also shown in Fig. 2 for the spinel structures.

Shear constants of spinel oxynitride

We can obtain the three cubic elastic constants $c_{1,1}$, $c_{1,2}$, and $c_{4,4}$ by appropriate deformation of the cubic unit cell,

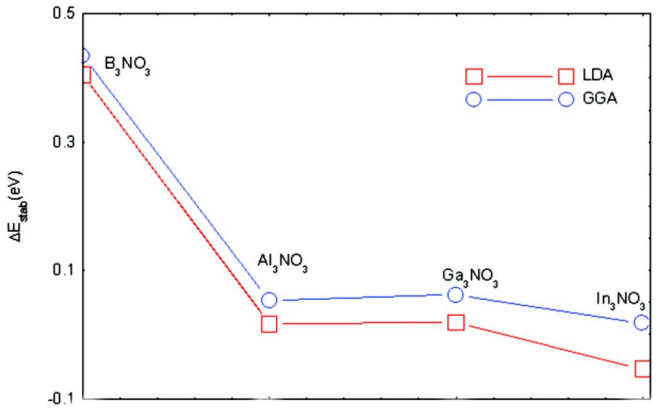

FIG. 3. (Color online) Relative stability of M_3NO_3 spinels as compared with lowest energy ambient phases of M_2O_3 and MN structures, as indicated in Table V.

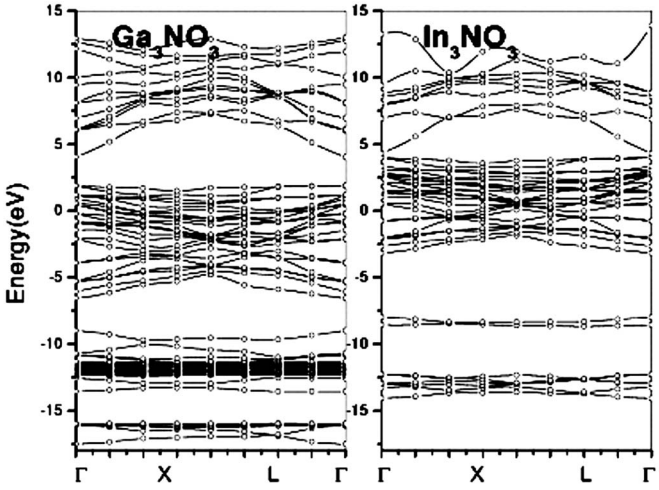

FIG. 4. Calculated energy band structure of Ga_3NO_3 and In_3NO_3 using a 56-atom cell.

and these are shown in Table IV. From these, we can deduce harmonic values of the bulk modulus and effective Voigt shear G using the well-known expressions

$$B = \frac{1}{3}(c_{1,1} + 2c_{1,2}) \quad G = \frac{1}{5}(c_{1,1} - c_{1,2} + 3c_{4,4})$$

and Young modulus and Poisson ratio

$$E = \frac{9BG}{3B+G}, \quad \nu = \frac{(3B-2G)}{2(3B+G)}$$

As with the equation of state bulk modulus, steady increases in the bulk and shear moduli are apparent in going from to B_3NO_3 to In_3NO_3. However, a tetragonal elastic instability of B_3NO_3 is found when the value of $(c_{1,1}-c_{1,2})$ was calculated. This rather surprising result was checked both for the size of calculational displacement in the appropriate distortion of $(c_{1,1}-c_{1,2})$ and for the usual convergence criterion. It would thus appear that while being a highly incompressible structure, B_3NO_3 is unstable against tetragonal displacement. It is likely that this instability is associated with strong covalent bonding interactions between the B-N and B-O structures that are evident in the tetragonal direction of the spinel unit cell of B_3NO_3.

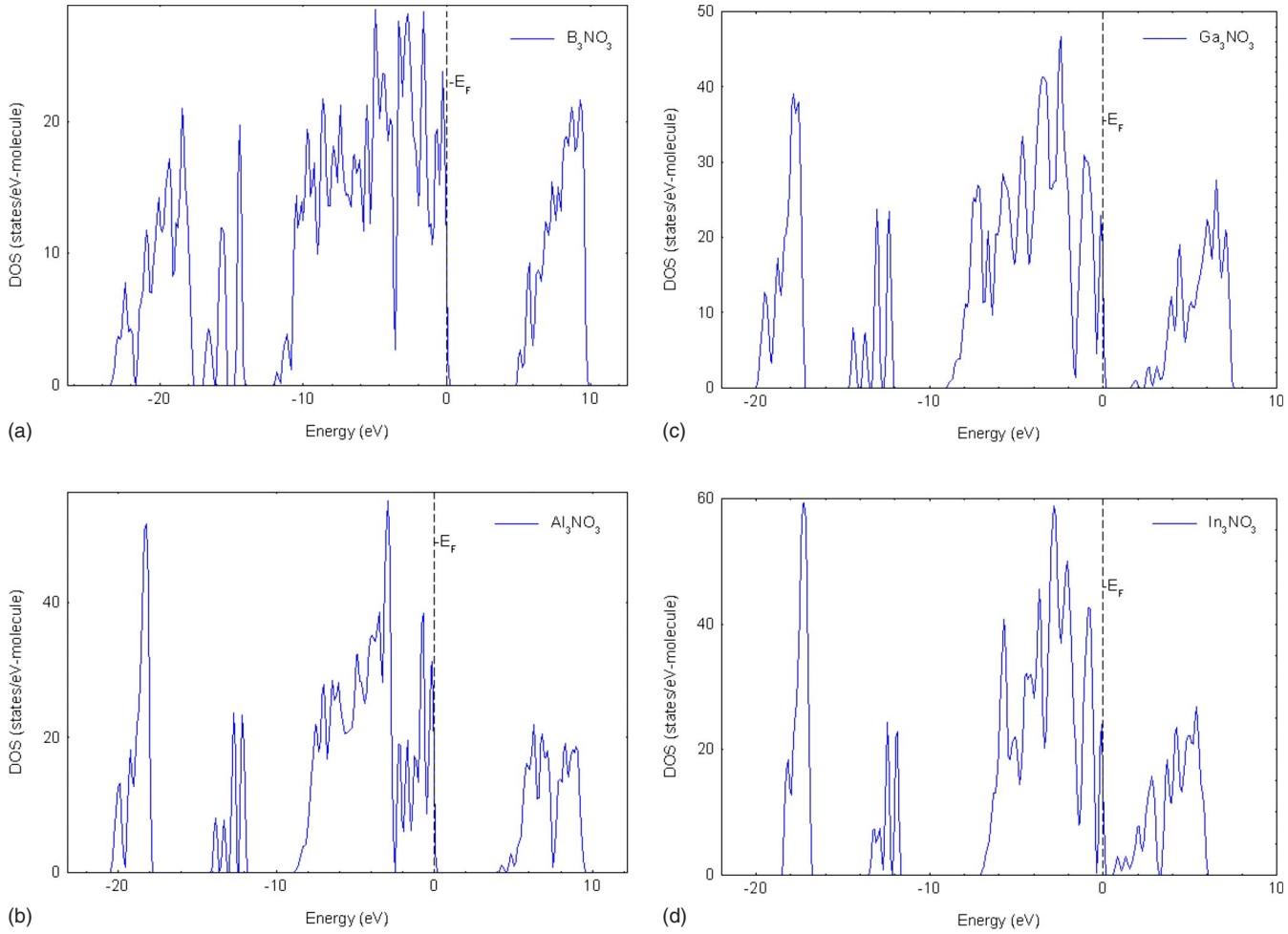

FIG. 5. (Color online) Calculated (LDA) density of state of the spinel structures; the Fermi energy level is at zero energy.

TABLE VI. Calculated band gaps of the spinels and their respective cubic binary nitrides.

	Band gap (eV)			Band gap (eV)		
Spinel	LDA	GGA	Nitride	LDA	GGA	Expt. (eV)[a]
B_3NO_3	4.60	4.43	*c*-BN	4.47	4.40	6.1–6.4
Al_3NO_3	4.02	3.70	*c*-AlN	3.10	3.09	4.5–6.2
Ga_3NO_3	1.72	1.37	*c*-GaN	1.97	2.43	3.30
In_3NO_3	0.40	0.40	*c*-InN	0	0	1.9–2.0

[a]Reference 44.

C. Relative stability

The relative stability of the spinels, M_3NO_3, have been estimated with respect to the simple mixture of each of its constituent phases. A measure of the relative stability of the spinel without any application of extreme conditions, such as pressure or temperature, is defined as

$$\Delta E_{stab} = E_{tot}[M_3NO_3] - E_{tot}[MN] - E_{tot}[M_2O_3] \quad (1)$$

where M represents B, Al, Ga, and In. In the above equation, E_{tot} is the total energy at the optimized geometry and corresponds to the free energy of the compound at zero temperature and zero pressure. ΔE_{stab} represents the relative stability of the spinels, M_3NO_3. A spinel with a positive value of ΔE_{stab} is likely to be metastable under ambient conditions, i.e., zero pressure and temperature, whereas a negative value of ΔE_{stab} suggests that the spinel phase would be stable.

In Table V, we give the calculated values for each of the family of oxide and nitride structures considered here. At this stage, it is to be noted that these values will have some degree of calculational uncertainty—conservatively estimated to be about 0.05 eV/atom. However, it is noted that there is a variation of ΔE_{stab}, depending on the component phases. The trend in the relative stability is shown in Fig. 3 for the lowest energy components indicated in Table V.

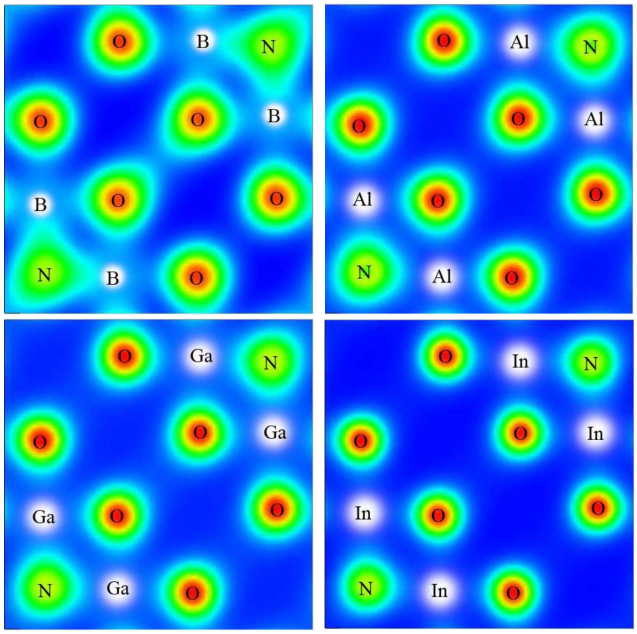

FIG. 6. (Color online) Calculated charge density distribution in the 001 plane of the spinel structure. The covalent bonding steadily increases from B to In, especially with N.

D. Electronic properties of the spinel structure

The energy band structure for Ga_3NO_3 has been discussed earlier,[25,58] and in Fig. 4, we now show the band structure for this material and for the In_3NO_3 structure. Both these materials have direct energy gaps in the 56-atom unit cell and thus have potentially important optoelectronic potential. In the 56-atom unit cell, the top of the valence band is relatively flat. However, there is a significant k dispersion in the conduction bands. In Fig. 5, we now show the calculated density of states for each of the spinel structures. Again, we see a trend—namely, that the energy gap is being steadily reduced from the B-related structure to the In-related structure.

The calculated energy band gaps are summarized in Table VI where comparison is also made with the energy band gap deduced for the binary zinc-blende nitride structures. We recall that both LDA and GGA underestimate the band gap due to the approximate nature of DFT functionals so the actual band gaps of the spinels should be larger than the calculated values given in Table VI.

We have seen earlier that the compressibility and elastic constants increase from the B_3NO_3 to the In_3NO_3 spinel. The reason for this is directly attributed to the reduction in covalent bonding from B_3NO_3 to In_3NO_3. This variation is evident from the charge density distribution on the spinel structures, shown in Fig. 6. In B_3NO_3, we note that B is bonding preferentially to N although simultaneously there appears some evidence of the formation of a O-O bond.

V. CONCLUSION

We have presented an investigation of an oxynitride spinel phase of the form M_3NO_3, where M=B, Al, Ga, or In. Structural and electronic properties have been examined. To date, only Ga_3NO_3 has been synthesized, and we now suggest that other spinel structures should be considered for use as possible materials. There is a definite trend—an increase—in the bulk and shear modulii when going from B to In. However, in addition, there is an abrupt reduction in the elastic constants of the B_3NO_3 spinel, the latter effect

probably being attributed to the asymmetric nature of B-O and B-N strong bonding in the B_3NO_3, leading to a tetragonal elastic instability. All results imply that spinels considered here are quite incompressible structures and, based on this and the calculated values of shear, Al_3NO_3 could especially be a hard material with possible applications. The energy band gaps of the spinels M_3NO_3 decrease systematically as M is changed from B to In. As with GaN and InN, the possibility that such spinel structures in the form M_3NO_3 could have interesting applications as an optoelectronic material should be considered.

ACKNOWLEDGMENTS

We acknowledge support from the National Research Foundation (South Africa) and the University of the Witwatersrand. One of us (O.U.O.) also acknowledges some partial support from the African Institute of Mathematical Science.

[1] E. M. Yoshimura and E. G. Yukihara, Radiat. Meas. **41**, 163 (2006).
[2] D. Bacorisen, R. Smith, J. A. Ball, R. W. Grimes, B. P. Uberuaga, K. Sickafus, and W. T. Rankin, Nucl. Instrum. Methods Phys. Res. B **250**, 36 (2006).
[3] J. M. Recio, R. Franco, A. Martin Pendas, M. A. Blanco, L. Pueyo, and R. Pandey, Phys. Rev. B **63**, 184101 (2001).
[4] K. E. Sickafus, J. M. Wills, and N. W. Grimes, J. Am. Ceram. Soc. **82**, 3279 (1999).
[5] J. E. Lowther, M. Schwarz, E. Kroke, and R. Riedel, J. Solid State Chem. **176**, 549 (2003).
[6] A. Zerr, G. Miehe, G. Serghiou, M. Schwarz, E. Kroke, R. Riedel, H. Fuess, P. Kroll, and R. Boehler, Nature (London) **400**, 340 (1999).
[7] S. D. Mo, L. Ouyang, W. Y. Ching, I. Tanaka, Y. Koyama, and R. Riedel, Phys. Rev. Lett. **83**, 5046 (1999).
[8] W. Y. Ching, Shang-Di Mo, Isao Tanaka, and M. Yoshiya, Phys. Rev. B **63**, 064102 (2001).
[9] I. Tanaka, F. Oba, T. Sekine, E. Ito, A. Kubo, K. Tatsumi, H. Adachi, and T. Yamamoto, J. Mater. Res. **17**, 731 (2002).
[10] A. Zerr, R. Riedel, T. Sekine, J. E. Lowther, Wai-Yim Ching, and I. Tanaka, Adv. Mater. (Weinheim, Ger.) **18**, 2933 (2006).
[11] Z. Y. Chen, H. J. Xiang, J. Yang, J. G. Hou, and Q. Zhu, Phys. Rev. B **74**, 012102 (2006).
[12] M. Mattesini and S. F. Matar, Comput. Mater. Sci. **20**, 107 (2001).
[13] C.-M. Sung and M. Sung, Mater. Chem. Phys. **43**, 1 (1996).
[14] B. A. Cook, J. L. Harringa, T. L. Lewis, and A. M. Russell, Scr. Mater. **42**, 597 (2000).
[15] J. Hu, W. D. Fei, and C. K. Yao, J. Mater. Sci. **36**, 4817 (2001).
[16] E. M. Bringa, R. E. Johnson, and R. M. Papaleo, Phys. Rev. B **65**, 094113 (2002).
[17] T. Mathew, Ph.D. thesis, University of Pune, India, 2002.
[18] W. Y. Ching, S. D. Mo, I. Tanaka, and M. Yoshiya, Phys. Rev. B **63**, 064102 (2001).
[19] T. F. W. Barth and E. Posnjak, Z. Kristallogr. **82**, 325 (1932).
[20] E. J. W. Verwey and E. L. Heilman, J. Chem. Phys. **15**, 174 (1947).
[21] W. Y. Ching, S. D. Mo, L. Ouyang, I. Tanaka, and M. Yoshiya, Phys. Rev. B **61**, 10609 (2000).
[22] D. Brasen, J. M. Vandenberg, M. Robbins, R. H. Willens, W. A. Reed, R. C. Sherwood, and X. J. Pinder, J. Solid State Chem. **13**, 298 (1975).
[23] M. Schwarz, G. Miehe, A. Zerr, E. Kroke, M. Heck, B. Thybusch, B. T. Poe, I. W. Chen, and R. Riedel, Angew. Chem., Int. Ed. **41**, 789 (2001).
[24] J. E. Lowther, M. Schwarz, E. Kroke, and R. Riedel, J. Solid State Chem. **176**, 549 (2003).
[25] K. C. Lo, H. P. Ho, K. Y. Fu, P. K. Chu, K. F. Li, and K. W. Cheah, J. Appl. Phys. **95**, 8178 (2004).
[26] P. Kroll, Phys. Rev. B **72**, 144407 (2005).
[27] O. M. Moon, B. C. Kang, and J. H. Boo, Thin Solid Films **464-465**, 164 (2004).
[28] D. Halil, S. Omer, S. I. Mehmet, and F. Hassan, Thermochim. Acta **445**, 1 (2006).
[29] M. Renzhi and B. Yoshio, Chem. Phys. Lett. **374**, 358 (2003).
[30] S. J. Hwang, C. Fernandez, J. P. Amoureux, J. Cho, and S. W. Martin, Solid State Nucl. Magn. Reson. **8**, 109 (1997).
[31] S. H. Jhi and Y. K. Kwon, Phys. Rev. B **71**, 035408 (2005).
[32] G. Simon, B. Hehlen, E. Courtens, E. Longueteau, and R. Vacher, Phys. Rev. Lett. **96**, 105502 (2006).
[33] J. Swenson and L. Börjesson, Phys. Rev. B **55**, 11138 (1997).
[34] G. E. Gurr, P. W. Montgomery, C. D. Knutson, and B. T. Gorres, Acta Crystallogr., Sect. B: Struct. Crystallogr. Cryst. Chem. **B26**, 906 (1970).
[35] C. T. Prewitt and R. D. Shannon, Acta Crystallogr., Sect. B: Struct. Crystallogr. Cryst. Chem. **B24**, 869 (1968).
[36] D. Nieto Sanz, P. Loubeyre, W. Crichton, and M. Mezouar, Phys. Rev. B **70**, 214108 (2004).
[37] G. Paglia, C. E. Buckley, A. L. Rohl, B. A. Hunter, R. D. Hart, J. V. Hanna, and L. T. Byrne, Phys. Rev. B **68**, 144110 (2003).
[38] R. S. Zhou and R. L. Snyder, Acta Crystallogr., Sect. B: Struct. Sci. **B47**, 617 (1991).
[39] M. Nieminen, L. Niinisto, and E. Rauhala, J. Mater. Chem. **6**, 27 (1996).
[40] S. Cho, J. Lee, I.-Y. Park, and S. Kim, Mater. Lett. **57**, 1004 (2002).
[41] C. Y. Wang, V. Cimalla, H. Romanus, T. Kups, G. Ecke, T. Stauden, and M. Ali, Appl. Phys. Lett. **89**, 011904 (2006).
[42] K. Kim, W. R. L. Lambrecht, and B. Segall, Phys. Rev. B **53**, 16310 (1996).
[43] K. Karch and F. Bechstedt, Phys. Rev. B **56**, 7404 (1997).
[44] K. Lawniczak-Jablonska, T. Suski, I. Gorczyca, N. E. Christensen, K. E. Attenkofer, R. C. C. Perera, E. M. Gullikson, J. H. Underwood, D. L. Ederer, and Z. Liliental Weber, Phys. Rev. B **61**, 16623 (2000).
[45] V. A. Gubanov, Z. W. Lu, B. M. Klein, and C. Y. Fong, Phys. Rev. B **53**, 4377 (1996).
[46] N. Nepal, K. B. Nam, J. Li, M. L. Nakarmi, and H. X. Jiang, Appl. Phys. Lett. **88**, 261919 (2006).
[47] E. Oh, J. Ho Choi, H.-K. Seong, and H.-J. Choi, Appl. Phys. Lett. **89**, 092109 (2006).

[48] S. P. Fu, T. J. Lin, W. S. Su, C. Y. Shieh, Y. F. Chen, C. A. Chang, N. C. Chen, and P. H. Chang, J. Appl. Phys. **99**, 126102 (2006).
[49] G. Kresse and D. P. Joubert, Phys. Rev. B **59**, 1758 (1999).
[50] J. P. Perdew and A. Zunger, Phys. Rev. B **23**, 5048 (1981).
[51] J. P. Perdew, K. Burke, and M. Ernzerhof, Phys. Rev. Lett. **77**, 3865 (1996).
[52] G. Kresse and J. Hafner, Phys. Rev. B **47**, 558 (1993).
[53] H. J. Monkhorst and J. D. Pack, Phys. Rev. B **13**, 5188 (1976).
[54] R. W. G. Wykoff, *The Structure of Crystals* (Interscience, New York, 1948).
[55] L. W. Finger and R. M. Hazen, J. Appl. Phys. **49**, 5823 (1978).
[56] C. Wolverton and K. C. Hass, Phys. Rev. B **63**, 024102 (2000).
[57] F. Birch, Phys. Rev. **71**, 809 (1947).
[58] E. Soignard, D. Machon, P. F. McMillan, J. J. Dong, B. Xu, and K. Leinenweber, Chem. Mater. **17**, 5465 (2005).
[59] P. Kroll, R. Dronskowski, and M. Martin, J. Mater. Chem. **15**, 3296 (2005).